Desalination and Water Treatment
www.deswater.com
doi: 10.5004/dwt.2019.24681

169 (2019) 49–58
November

Corrosion inhibition of mild steel in acidic solution by leaves and stem extract of *Acacia nilotica*

Fatma M. Mahgoub*, Ahmed M. Hefnawy, Eman H. Abd Alrazzaq

Materials Science Department, Institute of Graduate Studies and Research, Alexandria University, Egypt, email: ftm_mahgoub@alexu.edu.eg (F.M. Mahgoub)

Received 28 November 2018; Accepted 10 July 2019

ABSTRACT

Plant extracts have become vital as an eco-friendly and renewable resource for a wide range of corrosion inhibition applications. In this work, the inhibitive action of water extracts of *Vachellia nilotica* (VN) leaves and gum arabic (GA) stem of the *Acacia nilotica* on the corrosion of mild steel was studied using electrochemical measurements. The plant extracts were characterized by Fourier transforms infrared spectroscopy (FTIR), scanning electron microscopy, energy dispersive X-ray spectroscopy and also gas chromatography-mass spectrometry analysis to detect the majority of organic natural compounds in the extract. The adsorption of the inhibitor on mild steel surface was found to follow the Langmuir adsorption isotherm. Surface characterization by FTIR and SEM confirmed the formation of a protective layer on the mild steel surface. The efficiency obtained from the impedance data was around 89% for VN leaves and 86% for GA stem at 25°C. From these results, we conclude that VN leaves and GA stem show promising results as an eco-friendly and mild steel corrosion inhibitors.

Keywords: Adsorption; *Acacia nilotica*; Corrosion inhibition; Mild steel; Acidic solution

1. Introduction

Acidic solutions are utilized in industries for pickling [1–3]. Therefore, finding ways, to inhibit the corrosion rate has become the subject of recent studies [4,5]. The use of organic inhibitors is one of the effective ways to protect the metals, though most of them are costly and environmentally risky [6–16]. Therefore, the researchers' attention has been drawn towards finding low cost and safe inhibitors. The environmental friendly corrosion inhibitors were obtained from parts of plants such as root, seeds, leaves, stem and fruits [17–25].

Literature shows the use of plants as green corrosion inhibitors. Plant leaves, such as *Ananas comosus* leaves and olive leaves [26–31] are used to protect the metals. Tree *Acacia nilotica* was referred to as 'the tree of life', reflecting its healing nature. Mabberley [32] classified *Acacia nilotica* to belong to the family Fabaceae that is a commonly growing medium-sized tree (consists of leaves called *Vachellia nilotica* and stem called gum arabic). *Acacia nilotica* that was utilized in this study, (*Vachellia nilotica* leaves and gum arabic stem) has several organic compounds that have corrosion inhibition property. To the best of our knowledge, no studies were reported using water extracts of VN and GA as corrosion inhibitors for metals. The objective of our study is to analyze the efficiency of VN and GA extracts to be used as green corrosion inhibitor.

2. Experimental

2.1. Metal specimens

The samples utilized in the present study with the chemical composition (wt%) of C 0.37%, Mn 1.21%, P 0.0.21%, Si 0.23%, Cr 0.02%, Cu 0.016%,S 0.017%, V 0.003% and the reminder of the weight percentage is Fe, which was abraded with 600–1,200 grade emery papers, were washed with distilled water and dried with acetone.

* Corresponding author.

2.2. Preparation of plant extract

Stock solutions of the inhibitors were prepared by soaking the dried VN plant leaves (50 g) and GA stem (50 g) individually in deionized water (100 mL) for 24 h. The VN extract was filtered to get the desired concentrations (10, 30, 40 and 50 ppm) while for GA extract (40, 50, 70 and 80 ppm) and these concentrations were tested in H_2SO_4 (0.5 M) [33].

2.3. Electrochemical measurements

The electrochemical cell was composed of three electrodes: working electrode (WE) of surface area 1 cm^2, platinum electrodes (PE) act as the counter electrode and saturated calomel electrode (SCE) was used as the reference electrode (RE). Gamry PCI4G750 Potentiostat/Galvanostat/ZRA applications were used for potentiodynamic polarization and electrochemical impedance spectroscopy (EIS) measurements.

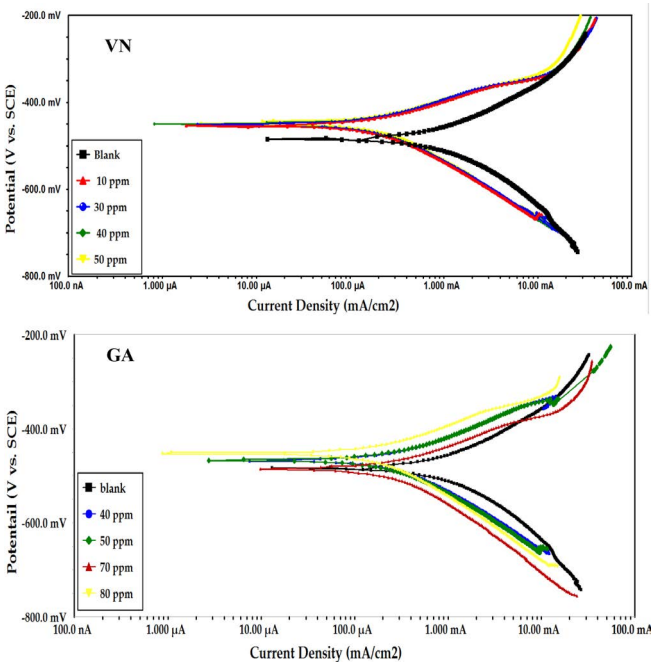

Fig. 1. Tafel curves for MS of different concentrations of VN or GA at 25°C.

For potentiodynamic polarization experiments, the potential was adjusted in the range of –250 to 250 mV relative to the open circuit potential. The scan rate of 1 mV/s at aerated 0.5 M H_2SO_4. Impedance measurements were performed at open circuit potential over a frequency range of 30 kHz to 0.1 Hz with 10 mV peak-to-peak -to-top amplitude, with AC signal [34].

2.4. Surface morphology

Scanning electron microscope (SEM; JEOL JSM-5500, Japan), Energy dispersive X-ray spectroscope (EDX) and Fourier transform infrared spectroscope (FTIR) were used to study surface morphology.

2.5. GC-MS analysis

A gas chromatograph-mass spectrometer (GC-MS) model 2014 (Agilent Technologies, Singapore) was used for the analysis of the extracts of leaves (VN) and the stems (GA) of the *Acacia nilotica* plants. The preparation of VN and GA was done by taking 1 g of extractions, mixed with 10 mL of methanol and was left for 1 h. The GC-MS mass spectra and data generated were analyzed, and the compounds and chemical functional groups present were identified [35,36].

3. Result and discussion

3.1. Electrochemical results

3.1.1. Polarization measurements

The Tafel plots for the MS in H_2SO_4 (0.5 M) alone and in presence of VN or GA extracts are given in Fig. 1. The data show that the extracts shifted the E_{corr} to more anodic side. The Tafel slopes (β_a and β_c) have slightly changed indicating that the protection occurred easily through covering the surface and the corrosion mechanism of the two inhibitors does not cause significant change.

Tafel parameters as β_a, β_c, E_{corr}, i_{corr}, were recorded in Table 1 with their %IE. The values of corrosion protections were calculated according to Eq. (1) as follows:

$$\%IE = \frac{i^0_{corr} - i_{corr}}{i^0_{corr}} \times 100 \quad (1)$$

Table 1
Polarization parameters of the mild steel electrode without and with inhibitors in acidic medium at 298 K

Inhibitor	C ppm	$-E_{corr}$ (mV)	i_{corr} (μA cm^{-2})	β_a (mV dec^{-1})	$-\beta_c$ (mV dec^{-1})	IE%
	Blank	484	692	98	101	0
VN	10	451	308	85	105	55.4
	30	450	98	52	86	85.8
	40	450	81	40	58	88.2
	50	447	76	55	69	89.1
GA	40	468	385	97	137	44.3
	50	467	221	67	103	68.1
	70	450	213	76	101	73
	80	452	196	73	132	80

where i^0_{corr} and i_{corr} are the corrosion current density in the absence and presence of the inhibitor, respectively.

The results showed a shift in E_{corr} values compared with the blank, which are less than 85 mV in our study via two inhibitors and the shift the anodic and cathodic curves towards lower current density give support to the mixed type inhibition nature of VN and GA. This means that it is affecting both anodic (metal dissolution) as well as cathodic (hydrogen evolution) reactions [37,38].

Table 1 shows that with the increase in concentration of inhibitors, the value of the current density decreases. This indicates that the inhibitor reduces the corrosion rate. The protection increases with increasing the concentration of the extracts in the medium [39].

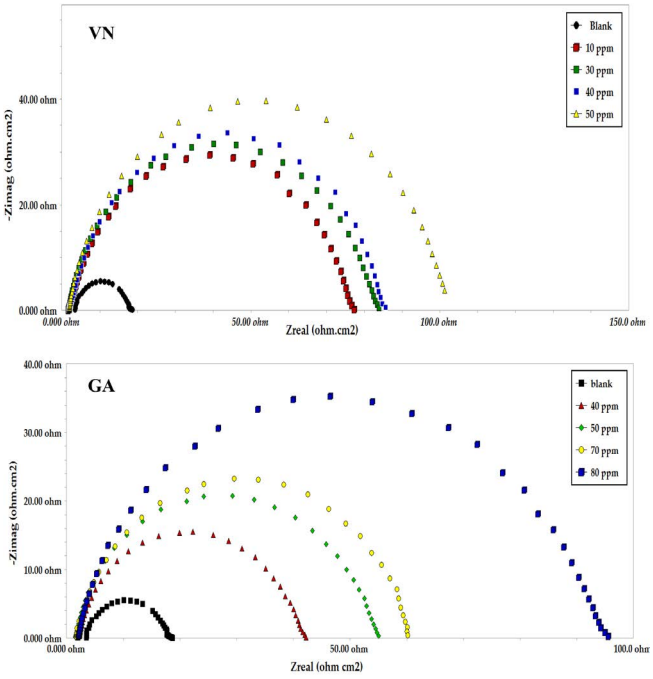

Fig. 2. Nyquist diagrams for MS containing different concentration of VN or GA at 25°C.

3.1.2. Impedance measurements

The results obtained from the polarization were further confirmed by impedance spectroscopy. The EIS measurements were carried out to study the capacitance double layer and metal dissolution that may occur on the metal surface without and with the inhibitors. Fig. 2 shows Nyquist plots via equivalent circuit includes the solution resistance (R_s) and double layer capacitance (C_{dl}) as shown in Fig. 3. The Nyquist plots are shown in Fig. 2 for the MS electrode in 0.5 M H_2SO_4 solution at room temperature without and with different amount of the inhibitors VN and GA at the respective open circuit potential. The plots reveal that the corrosion process is under activation control. Fig. 2 shows that there is a semicircle, indicating the charge transfer process during the corrosion process [40]. Table 2 reveals that the addition of the inhibitors, VN and GA, increases the values of R_{ct} and reduces the value of C_{dl}. The increase in R_{ct} value is attributed to the formation of the protective layer on the electrode/electrolyte interface [41]. The decrease in C_{dl} indicates an increase in the electric double layer thickness, which leads to an increase of the adsorption of the protective layer on the metal surface [42].

The protection percentage (%IE) was calculated as follows:

$$\%IE = \frac{R_{ct} - R^0_{ct}}{R_{ct}} \times 100 \quad (2)$$

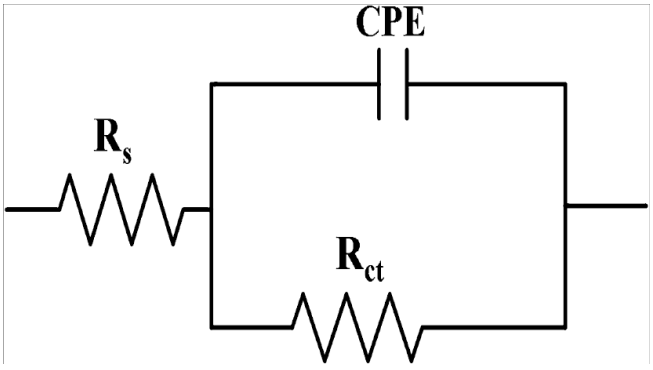

Fig. 3. Equivalent circuit to fit the impedance data.

Table 2
Impedance parameters for MS in 0.5 M H_2SO_4 solutions without and with inhibitors

Inhibitor	C ppm	R_s (Ω cm²)	C_{dl} (μF cm⁻²)	R_{ct} (Ω cm²)	IE%
VN	Blank	4.999	114.7	11.14	–
	10	1.829	44.80	70.24	59.4
	30	1.326	37.50	71.57	85.7
	40	1.308	26.01	89.86	86.4
	50	1.205	21.98	99.45	88.8
GA	40	2.382	56.07	47.34	44.8
	50	2.340	41.05	59.27	79.1
	70	1.964	39.12	61.36	79.6
	80	1.057	27.66	88.92	86.6

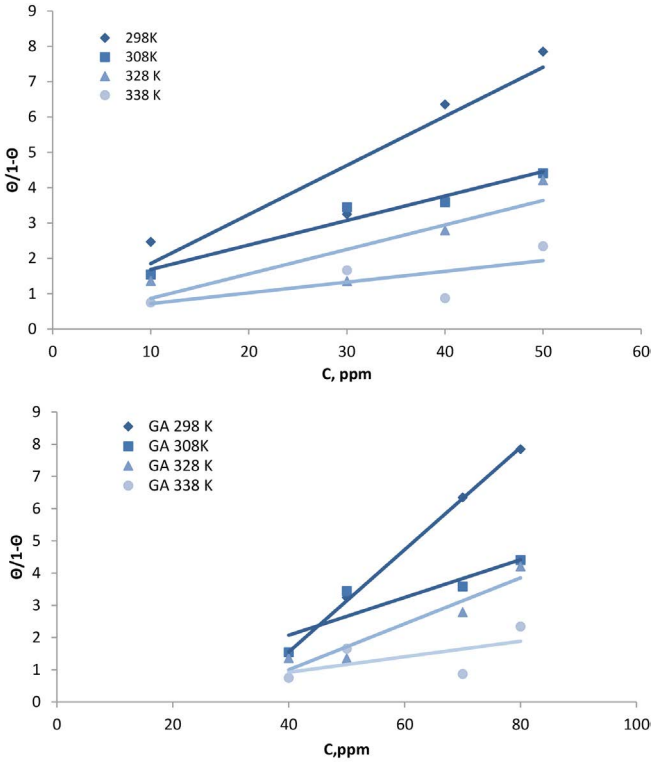

Fig. 4. Langmuir plots for VN or GA.

where R_{ct}^{0} and R_{ct} are the charge transfer resistances in the absence and presence of VN and GA extract, respectively.

The reduction of C_{dl} values indicate the reduction of the number of active sites required for metal dissolution due to displace of water molecules [40].

3.2. Adsorption isotherm

Surface coverage gives an insight into the inhibition mechanism. The adsorption isotherms describe the adsorbed inhibitor molecules on the surface [37]. Fig. 4 shows that VN or GA obey Langmuir adsorption isotherm for a plot of (θ/1–θ) vs. C_{inh} at various temperatures. The straight lines showed regression coefficients, r^2, close to unity, which successfully fits the Langmuir isotherm. The standard free energy change of the adsorption ΔG_{ads} was calculated from the adsorption equilibrium constant K_{ads} values according to Eq. (3):

$$\Delta G = -RT\ln(55.5K_{ads}) \tag{3}$$

where 55.5 mol/L was the molar concentration of water, R is the gas constant and T is the absolute temperature. Table 4 summarizes K_{ads} and ΔG_{ads} values at various temperatures.

$$\frac{\theta}{1-\theta} = K_{ads}C \tag{4}$$

Table 3 shows to the values of K_{ads} and the used temperatures. It is clear that there is an inverse relationship

Table 3
Data of the K_{ads} and ΔG_{ads} values at various temperatures

Inhibitors	Temperature (°K)	K_{ads} (L g^{-1})	r^2	$-\Delta G_{ads}$ (kJ mol^{-1})
VN	298	3.7×10^3	0.9626	30.31
	308	3.2×10^3	0.9714	30.94
	328	2.8×10^3	0.9858	32.59
	338	2.3×10^3	0.9934	33.03
GA	298	3.5×10^3	0.9413	30.16
	308	2.6×10^3	0.9677	30.42
	328	1.9×10^3	0.9798	31.54
	338	1.4×10^3	0.9883	31.64

Table 4
Kinetic parameters of mild steel in 0.5 M H_2SO_4 at various concentrations of inhibitors VN and GA

Concentration (ppm)		E_a (kJ mol^{-1})	ΔH^* (kJ mol^{-1})	$-\Delta S^*$ (kJ mol^{-1} K^{-1})
Blank		10.39	27.72	165.9
VN	10	41.57	43.68	175.2
	30	43.23	45.73	178.4
	40	48.23	49.88	180.2
	50	49.89	54.12	183.2
GA	40	26.61	28.37	172.5
	50	31.59	29.94	174.6
	70	35.76	33.26	177.2
	80	39.91	41.57	178.5

between the K_{ads} values and the temperatures. The adsorption of inhibitor has increased at low temperatures which allowed effective shielding and formation of a protective layer at the metal surface. Also, Table 3 shows that the free energy changes values are less than 40 kJ mol^{-1}, which confirms that the adsorption of inhibitor on the surface of steel is a physical adsorption. The adsorption took place via the electrostatic interaction of partially negative charged atoms of macromolecules with partially positively charged steel ions. This is assisted by the release of the adsorbed water molecules that enhanced the formation of a protective layer inhibiting the corrosive medium [40,43].

3.3. Activation energy

Data activation parameters can help understand the inhibitive mechanism of the additions. The activation energy at various concentrations of VN and GA extract were calculated from the plot of ln ($1/R_{ct}$) vs. 1,000/T using the following Arrhenius type Eq. (5):

$$\ln\left(\frac{1}{R_{ct}}\right)=\frac{-E_a}{RT}+\ln A \tag{5}$$

The Arrhenius plot for VN and GA extract in aqueous medium is displayed in Fig. 5. The values of Ea of VN and GA are calculated from slopes and the results are reported in Table 5.

Table 5 shows that the activation energy increases with the increase of the inhibitor's concentration VN and GA

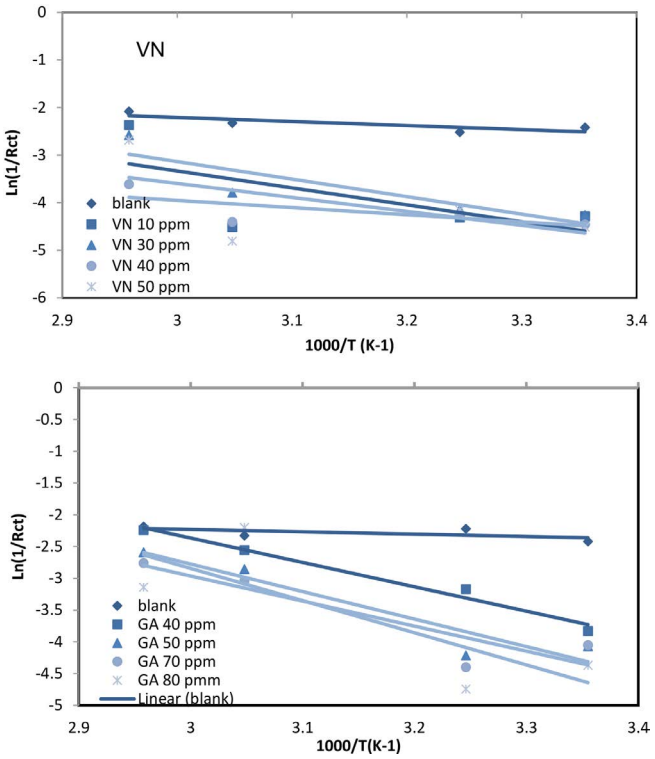

Fig. 5. Arrhenius plots of MS in 0.5 M H_2SO_4 of various concentrations of VN or GA at different temperatures.

[44]. When compared with the value of acid (10.39 kJ/mole) such increase is interpreted as the formation of an adsorption film. Mahgoub and AlRashdi [41] reported that the activation energy decreases with the increase in temperature. The decrease in activation energy may be attributed to an appreciable decrease in the adsorption of the inhibitor on the mild steel surface.

The ΔH^* and ΔS^* values were obtained from the following equation:

$$\rho=\frac{RT}{Nh}\exp\frac{\Delta S^*}{R}\exp\frac{-\Delta H^*}{RT} \tag{6}$$

where ρ is the corrosion rate ($1/R_{ct}$), h is the Planck's constant; N is the Avogadro's number; T is the absolute temperature and R is the universal gas constant. A plot of ln (ρ/T) vs. 1,000/T is illustrated in Fig. 6. The values of ΔH^* and ΔS^* were calculated from the slope ($\Delta H^*/R$) and intercept [ln(R/Nh) + ($\Delta S^*/R$)] of the straight lines in Fig. 6. The positive sign of ΔH^* indicates that the process is endothermic, which is reflected in slow dissolution of mild steel in the medium [18,45]. Thus, the inhibition efficiency decreases when the temperature rises. Table 4 shows that the E_a and ΔH^* are directly proportional to the increase in the concentration of the inhibitors. The entropy of activation is negative in both the uninhibited and inhibited systems. This can be attributed to the free movement of the inhibitor molecules in the bulk solution, which were adsorbed onto the metal surface, resulting in an increase in entropy [45]. This process may be enthalpy and entropic dependent as suggested by the change of ΔH^* and ΔS^* with the concentration of the inhibitor.

3.4. Surface characteraztion

Figs. 7a and b show the SEM images of the clean and corroded mild steel surface in sulfuric acid. Fig. 7b of MS in H_2SO_4 contains a large number of pits, while the surface looked much smoother in the presence of VN and GA inhibitors. This means that the inhibitors form a protective layer onto the surface of the metal and thus reduce the corrosion rate [46].

The EDX analysis of mild steel in 0.5 M H_2SO_4 only and in the presence of 50 ppm of the VN and of 80 ppm of the GA, portrays the spectra for the mild steel after immersion in the sulfuric acid solution. Fig. 8 shows a high O and Fe peak, indicating a high amount of oxygen and iron in the mild steel surface. A high Fe peak observable reflects a lower rate of iron dissolution in the medium containing the extracts [47].

The EDX spectra of the mild steel in sulfuric acid without and with inhibitors are also presented in Fig. 8. The spectra for the mild steel in 0.5 M H_2SO_4 solution (Fig. 8a) show a low Fe peak, indicating a low amount of iron in the steel surface due to acid dissolution. For the mild steel in H_2SO_4 solution (0.5 M) containing NV and GA extracts (Fig. 8b), a high Fe peak is observed compared with that in Fig. 8a, reflect a lower corrosion rate of iron.

The presence of O ion in the EDX for the mild steel in the acidic medium with the extracts (Fig. 8b) may be due to adsorption of active ingredients of extracts that is represented by the hydroxyl group on the steel surface.

Table 5
Various plant extracts that have been used in acidic medium

Medium	Inhibitor	Techniques	Results	IE%	# Ref
2 M HCl	*Aloe vera* leaves	Weight loss method	Langmuir adsorption Isotherm	67%	[17]
2 M HCl and 1 M H_2SO_4	1. *Ocimum viride slov* 2. *Telfairia occidantalis* 3. *Azadirachta indica* 4. *Hibiscus sabdariffa* (extract halide salts 0.5 M KCl and KBr)	Gasometric test at (30°C and 60°C)	Langmuir isotherm	87%	[19]
1 M HCl	*Acalypha torta* leaves (ethanol extract)	Weight loss, electrochemical chronocamperometric, SEM	Langmuir adsorption mixed type	90.38%	[20]
1 M HCl	*Caulerpa racemosa*	Weight loss, electrochemical UV, IR, NMR, AFM	Temkin adsorption	82%	[21]
1 M HCl	Papaveraceae (water extract)	Weight loss method, VU SEM	Langmuir adsorption	80%–92.5%	[24]
1 M HCl 0.5 M H_2SO_4	Petersianthus macrocarpus leaves	Electrochemical, gravimetry 313–333 K	Langmuir adsorption	61.3%–93.5%	[27]
1 M HCl H_2SO_4	*Laburnum watereri* Vossii leaves (ethanol extract)	Electrochemical, weight loss methods, FTIR, SEM	Freundlich adsorption anodic type	94%	[28]
1 M HCl	Pineapple leaves (ethanol extract)	Weight loss, hydrogen evalution 30°C–60°C	Langmuir adsorption	72%	[29]
1 M HCl	Bauhinia purpurea leaves	Electrochemical, weight loss, SEM	Langmuir adsorption mixed type	71%–89%	[30]
0.5 M H_2SO_4	1.*Vachella nilotica* (VN) 2.Gum arabic (GA) (water extract)	Electrochemical musearment SEM, EDX, FTIR, GC-MS 25°C–65°C	Langmuir adsorption mixed type	88.72% 86.6%	Our study

3.5. FTIR spectroscopy

Fig. 9 shows the FTIR spectra of VN and GA. The absorption of the broad bands at 3,427 and 3,434 cm^{-1} is assigned to OH and NH stretching virbrations, while the bands at 2,924; 2,932 and 2,859 cm^{-1} are attributed to the C–H strretching virbrations. The carboxyl groups C=O appear at 1,629 and 1,631 cm^{-1}.

The bands at 1,447 and 1,421 cm^{-1} may be due to OH and NH bending vibraions, while the C–O–C band appeared at 1,040; 1,069 and 566; 569 cm^{-1}. The C–H bending vibration is represented by the band observed at 1,201 cm^{-1}. It was found that the previous absorption bands coincided with the structures of VN and GA represented in Figs. 11 and 13 [43].

3.6. GC-MS analysis

Fig. 10 shows GC-MS spectrum of VN, which is characterized by eight peaks. Accordingly, the information of GC-MS spectrum shows that it quantitatively contains most of the following compounds: area% (8.12) of 1,2,3-benzentriol ($C_6H_6O_3$), 19.06% of ethanedioic acid, dihydrazide ($C_2H_6N_4O_2$), 1-butanol, 3-methyl acetate ($C_7H_{14}O_2$) and 14.24% of phenol, 2,6-dimethoxy ($C_8H_{10}O_3$), as the major chemical constituents. Structural assignment is based on spectral matching with NIST library (National Institute of Standards and Technology). The four main compounds of VN are as in Fig. 11.

Fig. 12 shows a GC-MS spectrum of GA, which is characterized with five peaks. Accordingly, the information of the

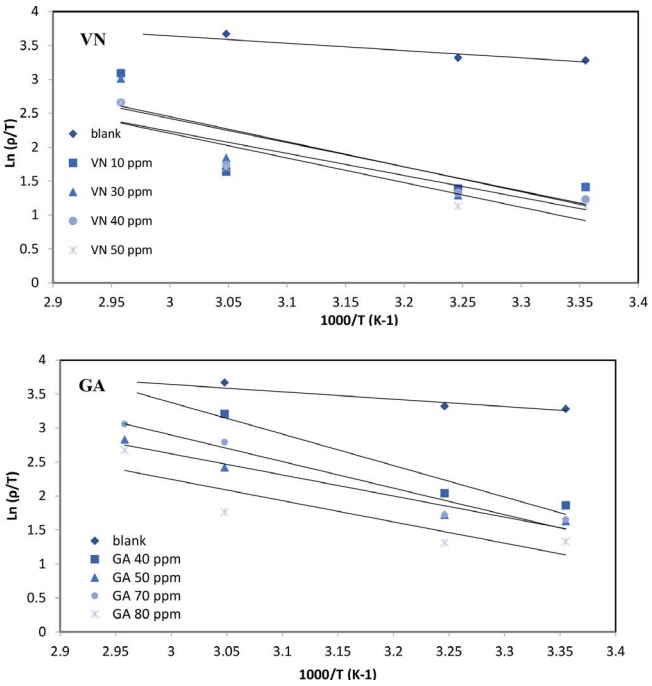

Fig. 6. Plot ln (ρ/*T*) vs. 1,000/*T* for inhibitors VN or GA on the MS in 0.5 M H_2SO_4.

GC-MS spectrum shows that quantitatively contains most of compounds: 8.348% of 9-octadecenoic acid(Z)-, methyl ester, 23.323% of methyl stearate; 26.591% gamma-sitosterol; 33.721% hexasiloxane, 1,1,3,3,5,5,7,7,9,9,11,11-dodecamethyl and 35.639% heptasiloxane, 1,1,3,3,5,5,7,7,9,9,11,11,13,13-tetradecamethyl as the major chemical constituents. The four main compounds of GA are shown in Fig. 13.

From the chemical structures of the studied compounds and functional groups reported by GC-MS and FTIR methods (Fig. 11 for VN) and (Fig. 13 for GA) was identified. The compounds fulfill basic requirements to be good corrosion inhibitors that contain aromatic or long carbon chain that has heteroatom(s) and conjugated systems [34,43].

3.7. Mechanism of inhibition

Our study showed that the green inhibitors (VN and GA) may form a film onto the steel surface through the physical absorption. The inhibitor mechanism in acidic medium may change due to some factors such as amount of the extracts and the type of the metal [47].

To show the effect of our extracts compared with other natural inhibitors, Table 5 shows the various plant extracts that have been reported in literature as corrosion inhibitor for mild steel in acidic medium. The green corrosion inhibitors (VN and GA) of our study were found to be effective

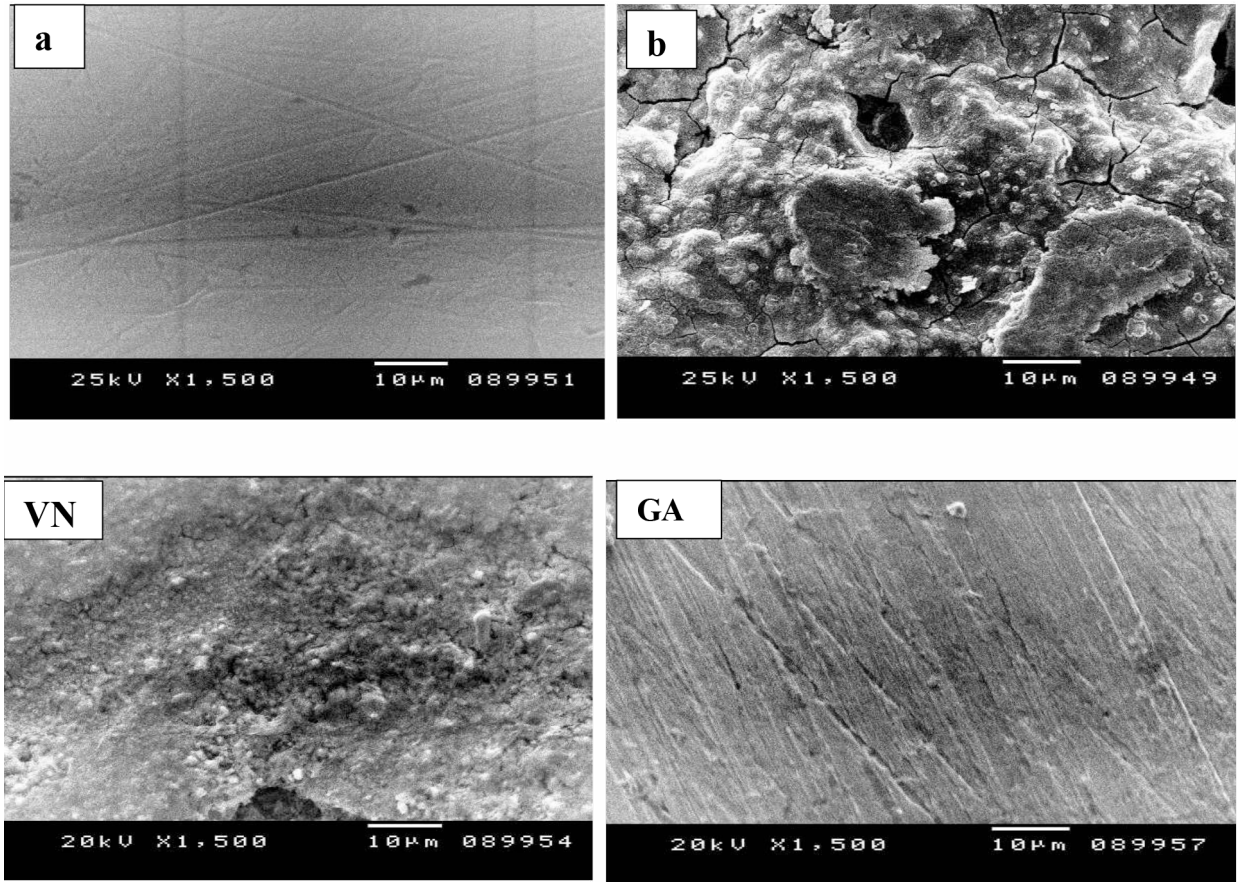

Fig. 7. SEM images of (a) mild steel; (b) mild steel in 0.5 M H_2SO_4; (c) mild steel with 50 ppm of VN for 24 h; (d) mild steel with 80 ppm of GA for 24 h.

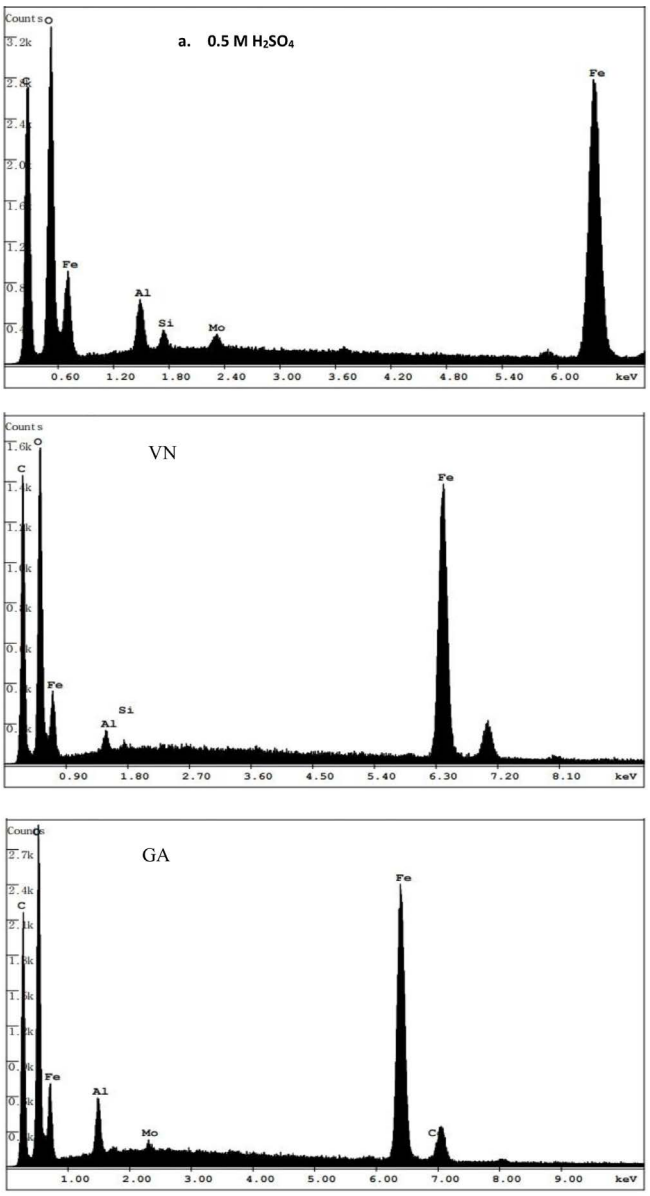

Fig. 8. EDX analysis on MS in (a) absence and (b) presence of inhibitors immersed for 24 h in 0.5 M H_2SO_4.

and produced inhibition in the range of 86%–88% and have a distinct advantage over toxic corrosion inhibitors. The results revealed that the protection of mild steel in acidic medium is concentration dependent and the protection was found to increase with increasing the concentration of inhibitors.

4. Conclusion

The investigated green corrosion inhibitors were effective for corrosion inhibition of steel in acidic medium. From this study, it can thus be concluded that the main mechanism of corrosion inhibition follows physical adsorption isotherms and obey Langmuir adsorption model. The percentage inhibition increases with the increase in the inhibitors concentration

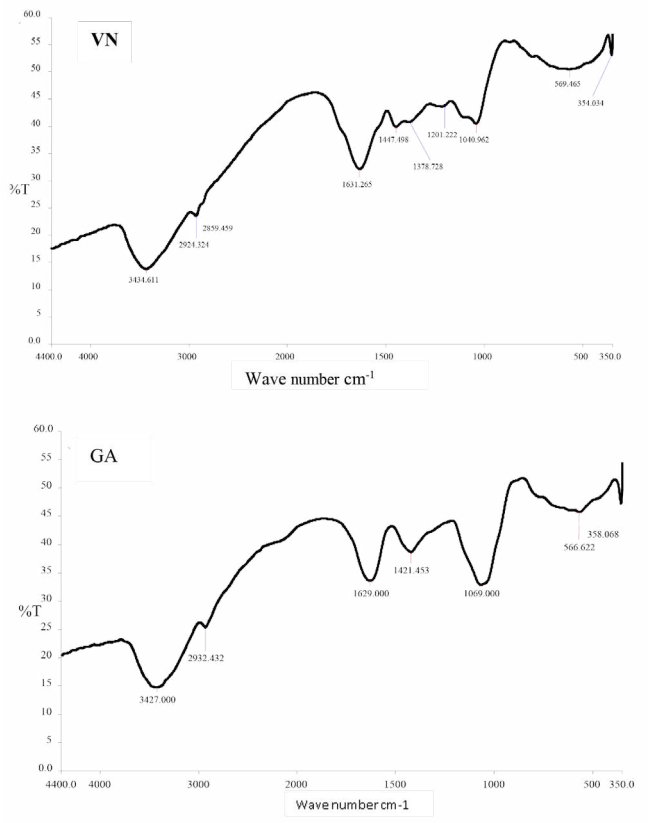

Fig. 9. FTIR spectroscopy of VN or GA extract.

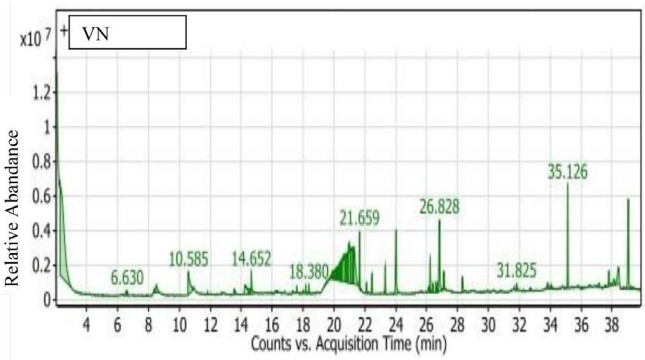

Fig. 10. GC-MS of VN.

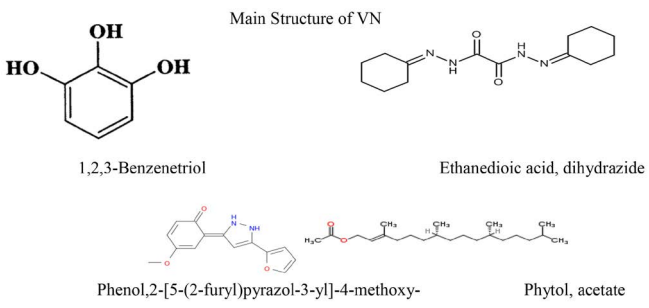

Fig. 11. Most of main structure of VN.

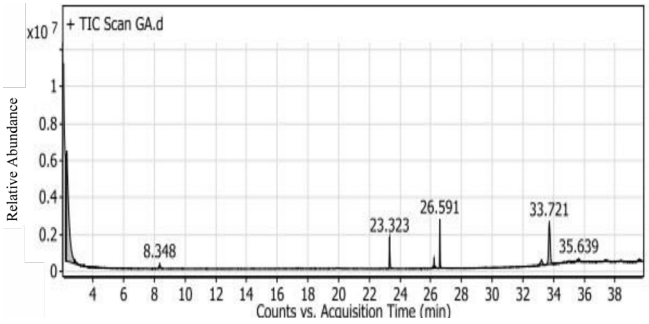

Fig. 12. GC-MS of GA.

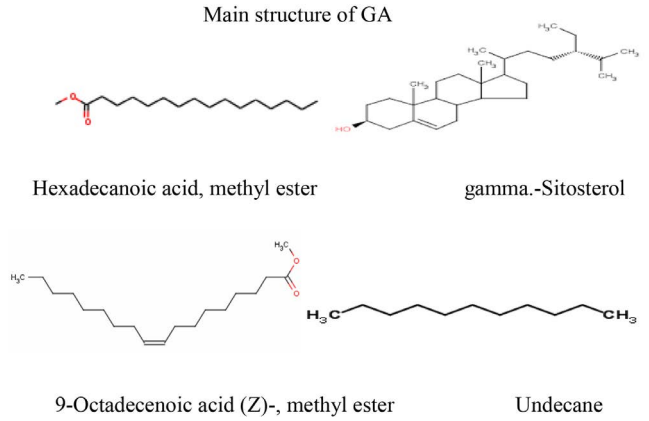

Fig. 13. Main structure of GA extracts compounds.

and decreases with an elevation of temperature. From thermodynamic values and activation energy, the negative data of (ΔG^* ads) and (ΔH^* ads) indicates that adsorption is spontaneous and exothermic. From the polarization data, the two inhibitors behaved as mixed-type inhibitors.

References

[1] V.V. Torres, R.S. Amado, C.F. De Sá, T.L. Fernandez, C.A. Riehl, A.G. Torres, E. D'Elia, Inhibitory action of aqueous coffee ground extracts on the corrosion of carbon steel in HCl solution, Corros. Sci., 53 (2011) 2385–2392.

[2] A. Ostovari, S. Hoseinieh, M. Peikari, S. Shadizadeh, S. Hashemi, Corrosion inhibition of mild steel in 1 M HCl solution by henna extract: a comparative study of the inhibition by henna and its constituents (lawsone, gallic acid, α-d-glucose and tannic acid), Corros. Sci., 51 (2009) 1935–1949.

[3] A.S. Fouda, S.A. Abd El-Maksoud, A. El-Hossiany, A. Ibrahim, Corrosion protection of stainless steel 201 in acidic media using novel hydrazine derivatives as corrosion inhibitors, Int. J. Electrochem. Sci., 14 (2019) 2187–2207.

[4] S. Banerjee, V. Srivastava, M. Singh, Chemically modified natural polysaccharide as green corrosion inhibitor for mild steel in acidic medium, Corros. Sci., 59 (2012) 35–41.

[5] H. Bentrah, Y. Rahali, A. Chala, Gum Arabic as an eco-friendly inhibitor for API 5L X42 pipeline steel in HCl medium, Corros. Sci., 82 (2014) 426–431.

[6] F.M. Mahgoub, A. Hefnawy, Inhibition mechanism of pitting corrosion of nickel in aqueous medium by some macrocyclic compounds, J. Phys. Chem., 4 (2012) 221–227.

[7] S.K. Shukla, M. Quraishi, R. Prakash, Polyanthranilic acid": an efficient corrosion inhibitor for mild steel in acidic solution, Corros. Sci., 50 (2008) 2867–2872.

[8] F.A. Ansari, C. Verma, Y.S. Siddiqui, E.E. Ebenso, M.A. Quraishi, Volatile corrosion inhibitors for ferrous and non-ferrous metals and alloys, Int. J. Corros. Scale Inhib., 7 (2018) 126–150.

[9] F. Bentiss, M. Traisnel, M. Lagrenee, The substituted 1, 3, 4-oxadiazoles: a new class of corrosion inhibitors of mild steel in acidic media, Corros. Sci., 42 (2000) 127–146.

[10] A.M.H. Othman, F.A. Binti Kassim, A.A.H. Kadhum, A.B. Mohamad, Synthesis and characterization of a novel organic corrosion inhibitor for mild steel in 1 M hydrochloric acid, Results Phys., 8 (2018) 728–733.

[11] M. Lashgari, A.M. Malek, Fundamental studies of aluminum corrosion in acidic and basic environments: theoretical predictions and experimental observations, Electrochim. Acta, 55 (2010) 5253–5257.

[12] K. Barouni, L. Bazzi, R. Salghi, M. Mihit, B. Hammouti, A. Albourine, S. El Issami, Some amino acids as corrosion inhibitors for copper in nitric acid solution, Mater. Lett., 62 (2008) 3325–3327.

[13] P.B. Raja, A.K. Qureshi, A.A. Rahim, H. Osman, K. Awang, *Neolamarckia cadamba* alkaloids as eco-friendly corrosion inhibitors for mild steel in 1 M HCl media, Corros. Sci., 69 (2013) 292301.

[14] S. Deng, X. Li, Inhibition by *Jasminum nudiflorum* Lindl leaves extract of the corrosion of aluminium in HCl solution, Corros. Sci., 64 (2012) 253–262.

[15] L. Herrag, B. Hammouti, S. Elkadiri, A. Aouniti, C. Jama, H. Vezin, F. Bentiss, Adsorption properties and inhibition of mild steel corrosion in hydrochloric solution by some newly synthesized diamine derivatives: experimental and theoretical investigations, Corros. Sci., 52 (2010) 3042–3051.

[16] G. Moretti, F. Guidi, F. Fabris, Corrosion inhibition of the mild steel in 0.5 M HCl by 2-butyl-hexahydropyrrolo [1, 2-b][1, 2] oxazole, Corros. Sci., 76 (2013) 206–218.

[17] O.K. Abiola, A. James, The effects of Aloe vera extract on corrosion and kinetics of corrosion process of zinc in HCl solution, Corros. Sci., 52 (2010) 661–664.

[18] T.K., Bhuvaneswari, V.S. Vasantha, C. Jeyaprabha, Pongamia Pinnata as a green corrosion inhibitor for mild steel in 1N sulfuric acid medium, Silicon, 10 (2018) 1793–1807.

[19] A.A. Ganash, F.M. Mahgoub, Electrochemical synthesis and corrosion performance of poly o-anisidine on 304 stainless steel, Prot. Met. Phys. Chem. Surf, 52 (2016) 555–561.

[20] G. Ji, P. Dwivedi, S. Sundaram, R. Prakash, Inhibitive effect of *Chlorophytum borivilianum* root extract on mild steel corrosion in HCl and H_2SO_4 solutions, Ind. Eng. Chem. Res., 52 (2013) 10673–10681.

[21] C. Kamal, M.G. Sethuraman, Caulerpin: a bis-indole alkaloid as a green inhibitor for the corrosion of mild steel in 1 M HCl solution from the marine alga Caulerpa racemosa, Ind. Eng. Chem. Res., 51 (2012) 10399–10407.

[22] S. Gaballah, N. Shehata, M. Shabaan, S. Noseir, A. Hefnawy, A. Hamed, Corrosion inhibition of aluminum in Hydrochloric acid solution using ceria doped polyvinyl chloride nanofiber, Int. J. Electrochem. Sci., 12 (2017) 1094–1105.

[23] S. Deng, X. Li, Inhibition by Ginkgo leaves extract of the corrosion of steel in HCl and H_2SO_4 solutions, Corros. Sci., 55 (2012): 407–415.

[24] G. Ji, S.K. Shukla, P. Dwivedi, S. Sundaram, R. Prakash, Inhibitive effect of *Argemone mexicana* plant extract on acid corrosion of mild steel, Ind. Eng. Chem. Res., 50 (2011) 11954–11959.

[25] K. Alaneme, S.J. Olusegun, A.W. Alo, Corrosion inhibitory properties of elephant grass (*Pennisetum purpureum*) extract: effect on mild steel corrosion in 1 M HCl solution, Alexandria Eng. J., 55 (2016) 1076–1076.

[26] L. Valek, S. Martinez, Copper corrosion inhibition by *Azadirachta indica* leaves extract in 0.5 M sulphuric acid, Mater. Lett., 61 (2007) 148–151.

[27] M.A. Quraishi, A. Singh, V. Singh, D.K. Yadav, K.S. Ashish, Green approach to corrosion inhibition of mild steel in hydrochloric acid and sulphuric acid solutions by the extract of *Murraya koenigii* leaves, Mater. Chem. Phys., 122 (2010) 114–122.

[28] R. Rajalakshmi, S. Subashini, A. Prithiba, Acid extracts of *Ervatamia coronaria* leaves for corrosion inhibition of mild steel, Asian J. Chem., 22 (2010) 5034–5040.
[29] U.F. Ekanem, S.A. Umoren, I.I. Udousoro, A.P. Udoh, Inhibition of mild steel corrosion in HCl using pineapple leaves (*Ananas comosus* L.) extract, J. Mater. Sci., 45 (2010) 5558–5566.
[30] N.S. Patel, S. Jauhari, G.N. Mehta, Mild steel corrosion inhibition by *Bauhinia purpurea* leaves extract in 1 N sulphuric acid, Arab. J. Sci. Eng., 34 (2009) 61.
[31] A.Y. El-Etre, Inhibition of acid corrosion of carbon steel using aqueous extract of olive leaves, J. Colloid Interface Sci., 314 (2007) 578–583.
[32] D.J. Mabberley, Mabberley's Plant-Book: A Portable Dictionary of Plants, Their Classification and Uses, 3rd ed., Cambridge University Press, 2008.
[33] E. Khamis, E. El-Rafey, A. Moustafa, A. Gaber, A. Hefnawy, N.Galal, S. El-Din, M. Salah El-Din, Comparative study between green and red algae in the control of corrosion and deposition of scale in water systems, Desal. Wat. Treat., 57 (2016) 23571–23588.
[34] X. Li, S. Deng, F. Hui, Inhibition of the corrosion of steel in HCl, H_2SO_4 solutions by bamboo leaf extract, Corros. Sci., 62 (2012) 163–175.
[35] M. Abdallah, E.A. Helal, A.S. Fouda, Aminopyrimidine derivatives as inhibitors for corrosion of 1018 carbon steel in nitric acid solution, Corros. Sci., 48 (2006) 1639–1654.
[36] Z. Cao, Y. Tang, H. Cang, J. Xu, G. Lu, W. Jing, Novel benzimidazole derivatives as corrosion inhibitors of mild steel in the acidic media. Part II: Theoretical studies, Corros. Sci., 83 (2014) 292–298.
[37] S. Deng, H. Fu, Three pyrazine derivatives as corrosion inhibitors for steel in 1.0 M H_2SO_4 solution, Corros. Sci., 53 (2011) 3241–3247.
[38] F.M. Mahgoub, F.M. Al-Nowaiser, A.M. Al-Sudairi, Effect of temperature on the inhibition of the acid corrosion of steel by benzimidazole derivatives, Prot. Met. Phys. Chem. Surf., 47 (2011) 381–386.
[39] I. Dehri, M. Ozcan, The effect of temperature on the corrosion of mild steel in acidic media in the presence of some sulphur-containing organic compounds, J. Phys. Chem., 98 (2006) 316–323.
[40] E.E. Oguzie, Evaluation of the inhibitive effect of some plant extracts on the acid corrosion of mild steel, Corros. Sci., 50 (2008) 2993–2998.
[41] F.M. Mahgoub, S.M. AlRashdi, Investigate the corrosion inhibition of mild steel in sulfuric acid solution by thiosemicarbazide, J. Phys. Chem., 6 (2016) 54–59.
[42] S. Lee lavathi, R. Rajalakshmi, *Dodonaea viscosa* (L.) leaves extract as acid corrosion inhibitor for mild steel–a green approach, J. Mater. Environ. Sci., 4 (2013) 625–638.
[43] E. Khamis, A. Hefnawy, A.M. El-Demerdash, Acid cleaning of steel using arghel echo friendly corrosion inhibitor, Materialwiss. Werkstofftech., 38 (2007) 227–232.
[44] N.A. Wazzan, F.M. Mahgoub, DFT calculations for corrosion inhibition of ferrous alloys by pyrazolopyrimidine derivatives, J. Phys. Chem., 4 (2014) 6–11.
[45] Obi. Egbedi, N.O. Essien, K.E. Obot, E.E. Ebenso, 1, 2-Diaminoanthraquinone as corrosion inhibitor for mild steel in hydrochloric acid: weight loss and quantum chemical stud, Int. J. Electrochem. Sci., 6 (2011) 913–930.
[46] G. Babaladimath, V. Badalamoole, S.T. Nandibewoor, Electrical conducting Xanthan Gum-graft-polyaniline as corrosion inhibitor for aluminum in hydrochloric acid environment, Mater. Chem. Phys., 205 (2018) 171–179.
[47] L.L. Shreir, R.A. Jarman, G.T. Burstein, Corrosion Metal Environment Reaction, Butterworth-Heinemann, London, 1994, pp. 4–160.